ISA Transactions 114 (2021) 251–262

Contents lists available at ScienceDirect

ISA Transactions

journal homepage: www.elsevier.com/locate/isatrans

Research article

Stationary wavelet transform based ECG signal denoising method

Ashish Kumar [a], Harshit Tomar [b], Virender Kumar Mehla [b], Rama Komaragiri [b], Manjeet Kumar [c,*]

[a] School of Electronics Engineering, Vellore Institute of Technology, Chennai, Tamil Nadu 600127, India
[b] Department of Electronics and Communication Engineering, Bennett University, Greater Noida, Uttar Pradesh 201310, India
[c] Department of Electronics and Communication Engineering, Delhi Technological University (DTU), Rohini, Delhi 110042, India

A R T I C L E I N F O

Article history:
Received 13 July 2020
Received in revised form 12 December 2020
Accepted 12 December 2020
Available online 15 December 2020

Keywords:
Electrocardiogram
Wavelet filter bank
Heart rate monitoring
ECG signal denoising
Stationary wavelet transform

A B S T R A C T

Electrocardiogram (ECG) signals are used to diagnose cardiovascular diseases. During ECG signal acquisition, various noises like power line interference, baseline wandering, motion artifacts, and electromyogram noise corrupt the ECG signal. As an ECG signal is non-stationary, removing these noises from the recorded ECG signal is quite tricky. In this paper, along with the proposed denoising technique using stationary wavelet transform, various denoising techniques like lowpass filtering, highpass filtering, empirical mode decomposition, Fourier decomposition method, discrete wavelet transform are studied to denoise an ECG signal corrupted with noise. Signal-to-noise ratio, percentage root-mean-square difference, and root mean square error are used to compare the ECG signal denoising performance. The experimental result showed that the proposed stationary wavelet transform based ECG denoising technique outperformed the other ECG denoising techniques as more ECG signal components are preserved than other denoising algorithms.

1. Introduction

Cardiovascular disease (CVDs) refers to various problems with heart or blood vessels, including heart attacks, heart failure, and stroke. According to the world health organization survey, nearly eighteen million human beings lose their lives each year [1]. Initial symptoms such as unexplained chest pain or exhaustion after moderate physical activity are frequently ignored. Thus, many patients are treated only after suffering from a heart attack or stroke. CVDs mainly occur because of the accumulation of plaque inside arteries, making the walls thicken and reducing the arteries' available cross-section area. As a result, the blood flow to organs and tissues reduces. As a result, to bring the blood flow to typical rates, the heart needs to pump more blood per unit time. Thus, the pressure on the heart increases. This inadequate blood supply rate sometimes ruptures heart muscles, which leads to myocardial infarction.

In many cases, CVDs are also due to the chronic inflammatory condition. Atherosclerosis is due to unhealthy eating habits, lack of exercise, a deposit of fats, cholesterol, and other substances present in the blood building up over many years inside the arteries. The primary investigation and diagnosis of CVDs are generally made with an ECG monitor.

The heart's conduction system controls the generation and propagation of electrical signals that cause the heart muscle to contract and the heart to pump blood. This electrical activity is measured by placing electrodes at specific points on the human body. The measured electrical activity from electrodes forms a composite recording in the form of a graph famously known as ECG [2]. Tracing the heart's resultant electrical activity consists of propagating many action potentials, as shown in Fig. 1. ECG is the most recognized tool for various biomedical applications, such as measuring heart rate, examining arrhythmia, diagnosing heart abnormalities, emotion recognition, and biometric identification [3]. For proper diagnostics of heart abnormalities, an ECG signal must be clean.

In most cases, ECG signals are not clean as noises and artifacts corrupt these signals. The primary sources of noise are poor contact between electrodes and skin, incorrect positioning of electrodes, activities of various muscles in the body, respiration, surrounding electrical equipment, and electronic devices used by the machine itself. Therefore, it is necessary to remove noises and artifacts so that ECG features can be examined efficiently and correctly. Some common noises are listed below.

1. **Baseline wandering**: It is a low-frequency noise from 0.15–0.3 Hz and is generally created by the patient's respiration or movements [3].

* Corresponding author.
E-mail addresses: akumar.1june@gmail.com (A. Kumar), HT67291@bennett.edu.in (H. Tomar), virender.mehla@gmail.com (V.K. Mehla), Rama.komaragiri@bennett.edu.in (R. Komaragiri), manjeetchhillar@gmail.com (M. Kumar).

https://doi.org/10.1016/j.isatra.2020.12.029
0019-0578/

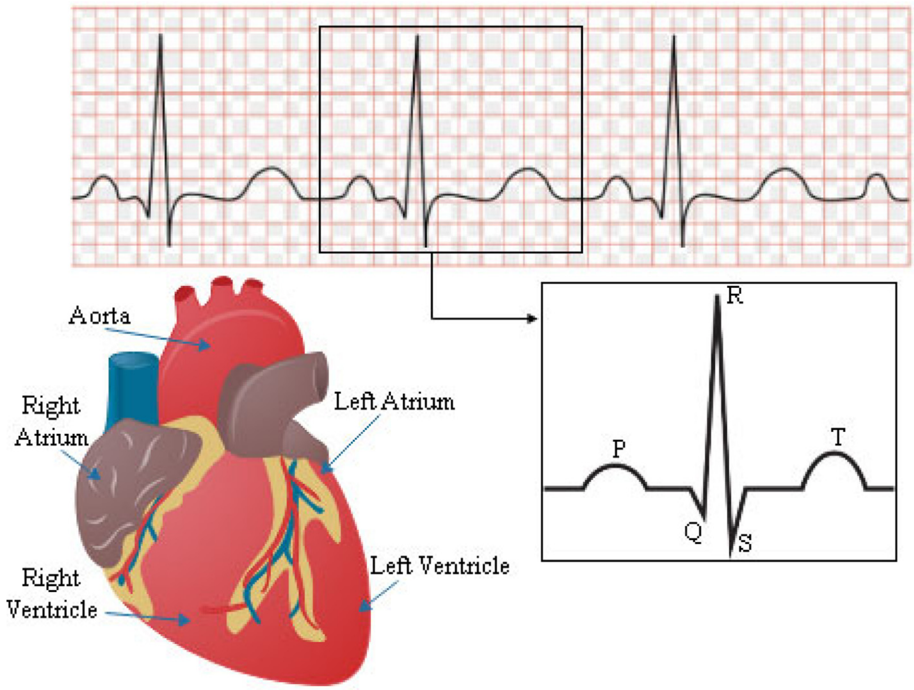

Fig. 1. Tracing of the overall electrical activity of the heart.

2. **Powerline interference**: It is a high-frequency noise in the frequency range of 50 Hz to 60 Hz, which is generally due to the power supply lines.
3. **Motion artifacts**: They are low-frequency noises that result from the displacement of electrodes placed on the skin and subject movement.
4. **Electromyogram Noise** (created by muscles): Electromyogram noise generally occurs due to muscle contraction and relaxation other than cardiac muscles and lies typically in the frequency range of 5–500 Hz [4].

Out of the noises given above, baseline wandering and powerline interference are the most prominent noises because baseline wandering occurs in the low-frequency region. In contrast, powerline interference occurs in the high-frequency region. These noises change some characteristics of the signal, which hinders proper diagnosis. Baseline wandering disturbs the ST segment period, one of the crucial parameters used in diagnosing CVDs [5]. Similarly, powerline interference completely overlaps the ECG signal's P and T waves, making the signal useless [6]. Thus, it is necessary to eliminate these noises without removing the features of the ECG signal. The proposed study aims to provide a comparative analysis of the most commonly used ECG denoising techniques.

In the literature, researchers presented various techniques to remove noises from the biological signals. Some of these techniques include highpass filters [7], lowpass filters [8,9], notch filters [10,11], adaptive filters [12,13], empirical mode decomposition (EMD) [14,15], wavelet transform (which mainly includes discrete wavelet transform (DWT) [16–21], stationary wavelet transform (SWT) [4], blind source separation method [22] and Fourier decomposition method (FDM) [23].

A highpass filter is used to remove baseline wandering noises, while the lowpass filter is used to remove powerline interference noises. While eliminating these noises, some critical features of the signal get eliminated. A notch filter effectively removes powerline interference noise. The notch filter's main disadvantage is its low-speed of computation and ringing due to the extended response. Zero-phase bi-directional filters compensate for the drawbacks of a notch filter [24,25].

Since notch filters are employed to remove a particular noise, adaptive filters are preferred over notch filters. Adaptive filters remove noise using a reference signal, which is highly correlated with the original signal. Due to the reference signal requirement, it is not a suitable technique in real-time applications. However, using some of the blind source separation methods, it is feasible to generate a reference signal without any implantable sensor, so incorporating both the blind source separation method and adaptive filtering could achieve good results. Another technique suitable to denoise an ECG signal in real-time is EMD. In EMD, a signal is decomposed into a set of amplitude and frequency modulated components commonly known as intrinsic mode functions (IMFs). IMFs denoise the signals. Using EMD, some low-frequency signals are discarded during the ECG signal's reconstruction, which leads to loss of valuable information [26]. The loss of some prominent features and the extraction of noise from corrupted ECG signals can be minimized using the Independent Component Analysis, an extensively used algorithm in the blind source separation method. Blind source separation methods generally operate on multiple ECG leads and are a very acclaimed technique for denoising biomedical signals. However, their high computational complexity leads to high power consumption and processing cost. Therefore, it is not a suitable algorithm for real-time monitoring in Holter ECG devices [4,27,28].

The methods that are feasible to denoise a non-stationary signal and bridge the shortcomings of the above methods are DWT and SWT, which work on wavelet decomposition, where coefficient thresholding is done to remove noise. These methods successfully remove the noises mentioned above, and the significant attributes of a signal are not affected.

This work proposes a procedure to select denoising algorithms suitable for real-time monitoring using comparative analysis. In this work, the proposed SWT method is quantitatively compared with existing methods by evaluating signal to noise ratio (SNR), the percentage-root-mean-square difference (PRD), and root-mean-square-error (RMSE). A clean ECG signal taken from the MIT-BIH Arrhythmia database is corrupted by adding noise. Then the denoising algorithm is applied to the corrupted ECG signal to get a denoised signal. The output PRD and RMSE values are calculated to depict the reconstructed and the reference signal's congruency in the subsequent stage. The robustness of the noise of an algorithm is investigated by checking out the improvement in SNR value. A comparison between the reference signal and the reconstructed signal obtained using SWT showed that the reconstructed signal entirely coincides with the reference or clean ECG signal, reflecting maximum output SNR and minimum PRD and RMSE values.

Hence denoising using SWT achieved a reconstructed signal with high visual quality and increased preservation of ECG signal components compared to other denoising algorithms. Further, the proposed denoising technique implemented using SWT retains the QRS complex's amplitude, while the existing denoising algorithms reduce the QRS complex's amplitude.

These remarkable results achieved by using the SWT algorithm makes it more suitable for hardware implementation with low computational complexity as denoising followed by detection of R-peaks becomes simple. R peak detection becomes a tedious job in other detection techniques as output alteration requires other techniques like derivative followed by thresholding to enhance and detect QRS Complex. As a result, computational complexity increases significantly. Further, SWT based denoising techniques can enable the ECG recording in noisy environments where the amplitude of the noise is high.

Thus, denoising techniques using SWT outperform the existing denoising techniques in terms of all three parameters: Robustness to noise, denoising performance, and computational complexity. SWT is generally a redundant transform where the output samples after decomposition by each level remain equal to the input. Correspondingly it is also a translation-invariant transform where down-sampling does not occur at each level. Hence, the SWT provides high efficiency as change detection and pattern recognition is generally not affected by transformed output, as in DWT. It is possible to analyze ECG signals in both the time and frequency domain using SWT as it is simple to analyze a non-stationary signal. In contrast, algorithms like highpass filter, lowpass filter, EMD, and FDM, it is not at all possible to analyze the ECG signal in both the time and frequency domain.

2. Existing methods to evaluate denoising performance

In this section, some of the previously used ECG denoising techniques are studied. A highpass filter is an electronic/digital filter that passes signals with a frequency higher than a specific cutoff frequency and attenuates signals with frequencies lower than the cutoff frequency. Similarly, a lowpass filter allows low-frequency signals and impedes high-frequency signals. The amount of attenuation for each frequency depends on the filter design. A lowpass filter mainly affects the amplitude of the QRS complex, and while a highpass filter changes the phase shift of the signal, hence bandpass filters are preferred.

Notch filter uses the properties of the highpass filter and lowpass filter, which was conceptualized by Weaver et al. [29]. Highpass and lowpass filters are used as components to implement notch filters in SWT and DWT. The notch filter is designed in such a way to reject a specific frequency band and to allow the remaining frequencies. Eq. (1) gives the transfer function of a notch filter.

$$H(s) = \frac{s^2 + \omega_0^2}{s^2 + \omega_R s + \omega_0^2} \tag{1}$$

Here, ω_0 is the central rejected frequency, and ω_R is the rejected bandwidth [30].

In [31], a notch filter's properties were modified to realize an all-pass filter, named infinite impulse response multiple notch filter. In [32], Kim deployed a novel idea for a notch filter by making a sharp notch filter using some unique coefficient equations, efficiently removing noises like PLI from the ECG signal. As the notch filter is not a suitable technique to denoise a signal with different noises; therefore, adaptive filters, EMD, and wavelet-based methods are preferred. Adaptive filtering is one of the most efficient methods used in denoising. It tends to track non-stationary signals. In [33], Widrow et al. introduced adaptive noise cancelation using primary input, which consists of a corrupted signal (clean signal + noise) and reference input, containing only an additional unknown noise. The unknown noise is treated so that the reconstructed signal is very similar to the primary input. After that, a newly constructed signal is subtracted from the primary input signal. The noise is eliminated without distortion of signal by taking care that both reference and primary input must coincide. If the input and reference signal does not match, combining two or more algorithms can result in phenomenal denoising results. In [34], IMEC's Cool Bio Digital Signal Processor was designed considering a wearable ECG for real-time monitoring. Here, two-algorithms, namely, electrode–tissue impedance with adaptive filtering and independent component analysis, are used to remove noises present in an ECG signal. Since adaptive algorithms mostly require an additional reference signal to denoise a signal, new ECG denoising techniques such as wavelet transform, EMD, and FDM are developed.

Wavelet transform is an alternative approach to Fourier transform and short-time Fourier transform as it can give both time–frequency components at any instant. At high frequencies, wavelet transform provides better time resolution, while at low frequencies, it provides better frequency resolution. Wavelet transform consists of a wavelet and a transform. In wavelet transform, wavelet or mother wavelet is a small oscillating wave that can change its finite window length and location depending upon translation parameter (b) and scaling parameters (k), as shown in Eq. (2) [35].

$$\psi_{b,k}(t) = \frac{1}{\sqrt{k}} \psi\left(\frac{t-b}{k}\right) \tag{2}$$

$\psi_{b,k}(t)$ is a function representing the mother wavelet, which is translated by the factor of "b" and scaled by the "k" factor. Convolution of a mother wavelet with a signal results in a wavelet transform. Generally, wavelet transforms are categorized as continuous wavelet transform (CWT) and discrete wavelet transform (DWT). Continuous wavelet transform is a convolution of the wavelet function $\psi(t)$ with the signal $x(t)$ and is given by Eq. (3).

$$\mathrm{CWT}(b,k) = \frac{1}{\sqrt{|k|}} \int_{-\infty}^{-\infty} x(t)\, \psi\left(\frac{t-b}{k}\right) dt \tag{3}$$

In CWT, scaling and translation parameters are continuous parameters, and due to which huge amount of wavelet coefficients are generated. The scales and positions of a CWT are chosen to be discrete to reduce the amount of data. The discretization simplifies the analysis and reduces the data size [36]. In a discrete wavelet transform, a mother wavelet function is selected to decompose and reconstruct a signal. Examples of some mother wavelets include Haar, Daubechies, biorthogonal, Morlet. The selection of wavelet transform is always highly correlated with the signal to get appropriate coefficients. In [37], Seljuq et al. compared and used the best-fitted mother wavelet to ensure that the ECG signal's critical information is retained. In DWT, coefficients are calculated at each decomposition level, which is equal to coefficients in the original signal, then coefficient thresholding is performed at each decomposition level. However, due

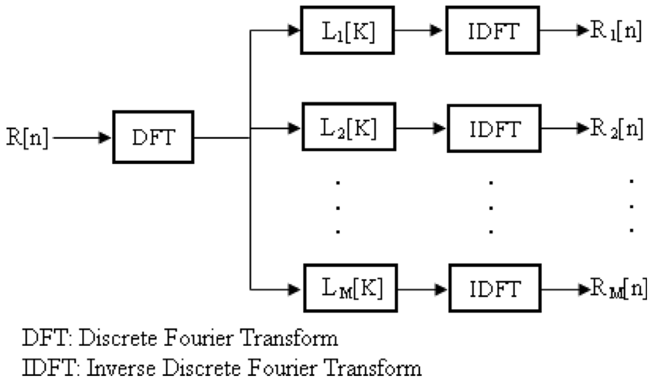

Fig. 2. Signal decomposition using FDM.

to subsampling at each decomposition level, DWT is a translation variant, affecting the output.

Therefore, its extended version, known as the stationary wavelet transform, is preferred. Stationary wavelet transform is almost similar to DWT and designed so that the output remains unaffected because of translation invariance. This translation invariance is achieved by avoiding the subsampling process. Hence, the number of output samples at each level is equal to the number of input samples [38]. Therefore, it is observed that SWT is more appropriate than DWT. Strasser et al. [38] used SWT to remove the complete QRS complex with P and T waves by applying thresholding at each SWT decomposition level. Further, a clean ECG signal is obtained by subtracting the difference between the original ECG signal and the reconstructed ECG signal from the noisy ECG signal.

Recently few decomposition techniques are also introduced, namely, EMD, FDM, to name a few. These techniques directly decompose the signal and perform denoising accordingly. Empirical mode decomposition (EMD) is an efficient approach for the analysis of non-stationary signals which decomposes a given signal, $a[n]$, into a finite number of intrinsic band functions (IMFs) $bi[n]$ and a residue $c[n]$, which is represented by Eq. (4) [39,40]:

$$a[n] = \sum_{k=1}^{M} b_i[n] + c[n] \tag{4}$$

Here M represents the number of IMFs. Each IMF must satisfy the following conditions:
(i) The difference in the number of zero-crossing and the number of peaks should differ by zero or at most differ by unity.
(ii) The average value of the lower and upper envelope should be zero at any instant of the complete duration of the given signal.
After segmenting the given signal into various IMFs, the next step is to extract the relevant features for denoising the biomedical signals such as ECG and EEG signals.

Fourier mode decomposition (FDM) is the recently developed signal decomposition procedure derived by Singh et al. in [41] to analyze non-stationary time-series data such as biomedical signals and earthquake data speech signals. By applying this technique, any signal, $R[n]$, can be represented in terms of a set of orthogonal basis functions, $R_1[n], R_2[n], \ldots R_M[n]$, commonly known as Fourier intrinsic band functions (FIBFs), which can be represented in Eq. (5) as follows:

$$R[n] = g_0 + \sum_{i=1}^{M} R_i[n] = g_0 + \sum_{i=1}^{M} g_i[n] \tag{5}$$

Where g_0 represents the average value of a signal, and $R_i[n]$ represents orthogonal basis functions with $i = 1, 2, 3 \ldots, M$. The block diagram representation of the FDM method by applying DFT based zero-phase filter bank is shown in Fig. 2. These FIBFs are local, adaptive, complete, and orthogonal, which satisfy the following conditions:

(i) FIBFs should have zero mean functions. i.e. $\int_p^q R_i(t)\,dt = 0$
(ii) FIBFs should satisfy the orthogonality condition. i.e. $\int_p^q R_i(t)\,R_k(t)\,dt = 0, \forall i \neq k$
(iii) FIBFs show analytical representation with instantaneous frequency and instantaneous amplitude, which is represented by $\omega_i(t) = \frac{d}{dt}\phi_i(t) \geq 0 \text{ and } a_i(t) \geq 0, \forall t$.

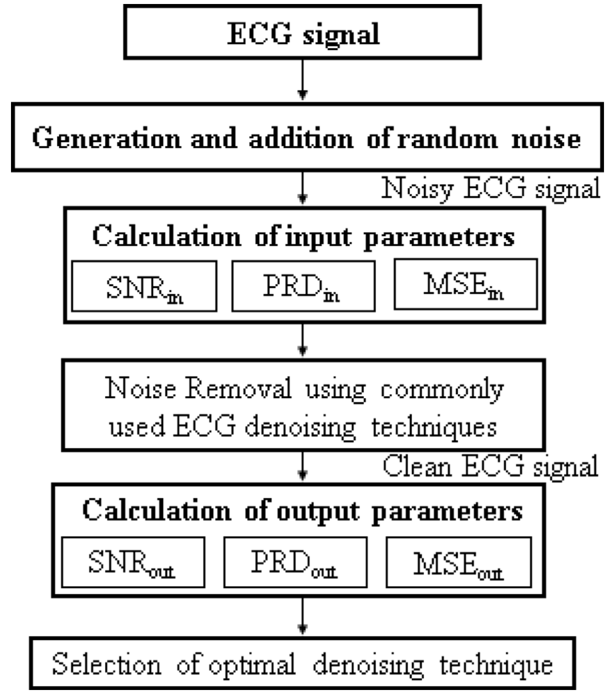

Fig. 3. An algorithmic structure used in ECG signal denoising.

3. Proposed method

The typical algorithmic structure used to select an optimal ECG signal denoising technique is shown in Fig. 3. In the present work, ECG signals from *physionet.org* are used as input [42]. As the ECG signals from [42] are available in raw form, they are assumed to be normalized and clean. By noting that the length of noise should be equal to that of the signal, a random noise source in the form of a sinusoidal signal of frequency 60 Hz is added to the normalized clean ECG signal.

The performance of the algorithm is compared by computing and comparing some input parameters and output parameters. After calculating input parameters, corrupted or noisy signals are applied to some commonly used denoising techniques: lowpass filter and highpass filter, Wavelet (discrete wavelet transform, and stationary wavelet transform), FDM, and EMD. These algorithms are used to recover the original ECG signal from an ECG signal corrupted with noise. The accuracy of denoising techniques is discussed by comparing different parameters of the denoised signal. In this work, MATLAB® R2020a *(The MathWorks, Inc., Natick, MA, USA)* environment is used. The following is a description of the proposed and other denoising techniques.

1. Lowpass Filter and Highpass Filter: lowpass filter and highpass filter with a cutoff frequency of 0.5 Hz–40 Hz are used

in the present work as the energy of the ECG signal (P-wave, QRS complex, and T-wave) lie in 0.5 Hz–40 Hz frequency range [43]. The difference equation of the lowpass filter and highpass filter used in the present work is as follows [44]:

$$H_1(z) = \frac{0.8576 - 0.032z^{-1} + 0.8629z^{-2} - 0.0811z^{-3}}{1 - 1.2096z^{-1} + 0.2644z^{-2} + 0.0144z^{-3}} \tag{6}$$

$$H_2(z) = \frac{-0.5034 + 1.9441z^{-1} - 1.9441z^{-2} + 0.5034z^{-3}}{1 - 1.1737z^{-1} + 0.2982z^{-2} + 0.0245z^{-3}} \tag{7}$$

2. Discrete Wavelet Transform: In DWT, the ECG signal is subsampled at each level, and simultaneously, the detail coefficients are subjected to denoising thresholds. Some thresholding schemes are hard threshold, adaptive threshold, soft threshold, sure shrink threshold, and universal threshold. Among the above thresholding techniques, adaptive thresholding is most suitable for ECG signal denoising [45]. After eliminating noise, finally, the inverse of DWT is performed to reconstruct the denoised ECG signal. In the present work, biorthogonal 3.1 wavelet transform with adaptive thresholding is used to decompose the noisy ECG signal.
3. Empirical Mode Decomposition Technique: EMD is employed on the noisy ECG signal. In the pre-processing stage, the data is normalized. Then, EMD decomposes a non-stationary time series into a finite number of intrinsic mode functions, which are monocomponent non-stationary signals. A total of six IMFs and residue components are achieved by employing EMD which is shown in Fig. 6(e).
4. Fourier Decomposition Method: A noisy ECG signal is decomposed into a set of monocomponent non-stationary signals by dividing the signal's complete bandwidth into an equal number of frequency bands. These monocomponent non-stationary signal frequency bands are known as Fourier intrinsic band functions (FIBFs). The maximum frequency of an ECG signal is calculated by dividing the sampling frequency by two. The maximum frequency is used to determine the cutoff frequency of each FIBF. FIBF should have zero mean function, which means the segmented ECG signal provides a zero DC level shift. The segmented ECG signal contains low and high-frequency components only. After determining FIBFs, various parameters like SNR, PRD, and MSE of each FIBF are competed. Eight FIBFs are extracted from the noisy ECG signal, and the output of the 8th FIBF is the denoised ECG signal.
5. Stationary Wavelet Transform: After the pre-processing, the input ECG signal is subjected to a series of a lowpass filter and highpass filter to reject the frequency band as per the Nyquist criterion. This method does not perform any subsampling or decimation. Hence, the length of both the signals produced from the lowpass filter and highpass filter remains the same. At each level, the signal is decomposed into detailed coefficients and approximate coefficients. The approximate coefficients are outputs of lowpass filters ($h_i[n]$), and detail coefficients are the outputs of highpass filters ($g_i[n]$). This process continues up to "n" decomposition levels [46]. The block diagram of SWT is shown in Fig. 4 [46].

The present work uses a biorthogonal 3.1 wavelet transform to decompose the input ECG signal using three decomposition levels known as wavelet filter banks. Detail coefficients (D_c), as well as approximation coefficients (A_c), are calculated at each decomposition level. Mathematically, D_c, and A_c can be computed in Eqs. (8) and (9), respectively [46].

$$\begin{aligned} A_{c_{b+1,k}} &= \int_{-\infty}^{\infty} 2^{-\frac{b+1}{2}} x(t)\phi^*\left(\frac{t-b}{2^{b+1}}\right)dt \\ &= \sum h[a]\, C_{b,k+2^b a} \end{aligned} \tag{8}$$

$$\begin{aligned} D_{c_{b+1,k}} &= \int_{-\infty}^{\infty} 2^{-\frac{b+1}{2}} x(t)\psi^*\left(\frac{t-b}{2^{b+1}}\right)dt \\ &= \sum g[a]\, C_{b,k+2^b a} \end{aligned} \tag{9}$$

Here, "b" is the translation parameter and "k" scaling parameter.

As SWT does not perform decimation, filters are accordingly modified to perform thresholding. After eliminating noise, finally, the inverse of SWT is performed to reconstruct the denoised ECG signal.

4. Results and discussion

In this section, various ECG denoising techniques, namely, lowpass filter, highpass filter, DWT, EMD, FMD, and SWT, are evaluated using four ECG databases. The four ECG databases used in this work are the MIT BIH Arrhythmia database, MIT-BIH Noise Stress Test database, Physionet PTB Diagnostic ECG Database, and QT database. These databases are publicly available at [42]. A brief description of these databases are as follows:

1. **MIT-BIH Arrhythmia database:** It includes a collection of 48 fragments obtained from 47 persons where two records were taken from the same person, and each fragment has a duration of 30 min. These recordings were taken from two-channel ECG and recorded by BIH Arrhythmia Laboratory between 1975 and 1979. These recordings have a sampling frequency of 360 Hz and are digitized using an 11-bit resolution over a 10-mV range [47].
2. **MIT-BIH Noise Stress Test database:** It consists of a total of 15 recordings, out of which 12 are half-hour ECG recordings, and rest 3 are typical noises viz. baseline wander, muscle noise (EMG), and electrode motion artifact. These noises are extracted from the recordings by selecting their interval, contaminated by noise [48].
3. **Physionet PTB Diagnostic ECG database:** It contains 549 recordings taken from 290 persons (aged 17–87). Each record consists of 15 concurrently measured signals. Each signal's sampling frequency is 1000 Hz, with a 16-bit resolution over a range of ±16.384 mV [49].
4. **The QT database:** It has a collection of totals of 105 recordings of fifteen minutes each, and these recordings are gathered from different other databases. These records were taken from two-channel ECG and sampled at a frequency of 250 Hz.

The denoising efficiency of the proposed method with the five other techniques is compared with some parameters at both the input stage (original ECG signal) and the output stage (denoised ECG signal). SNR, PRD, and RMSE [18] are the parameters used in this study. Signal to noise ratio (SNR) is the ratio of signal to noise and given by Eq. (10). The improvement in SNR, Improved SNR is given by Eq. (11).

$$\mathrm{SNR} = 10 \times \log_{10} \frac{\sum_{k=1}^{N}(y(k) - x(k))^2}{\sum_{k=1}^{N}(\hat{x}(k) - x(k))^2} \tag{10}$$

And

$$\text{Improved SNR} = \text{Output SNR} - \text{Input SNR} \tag{11}$$

Here $y(k)$ represents a corrupted ECG signal; $x(k)$ refers to a noise-free ECG signal while $\hat{x}(k)$ refers to the estimated signal obtained

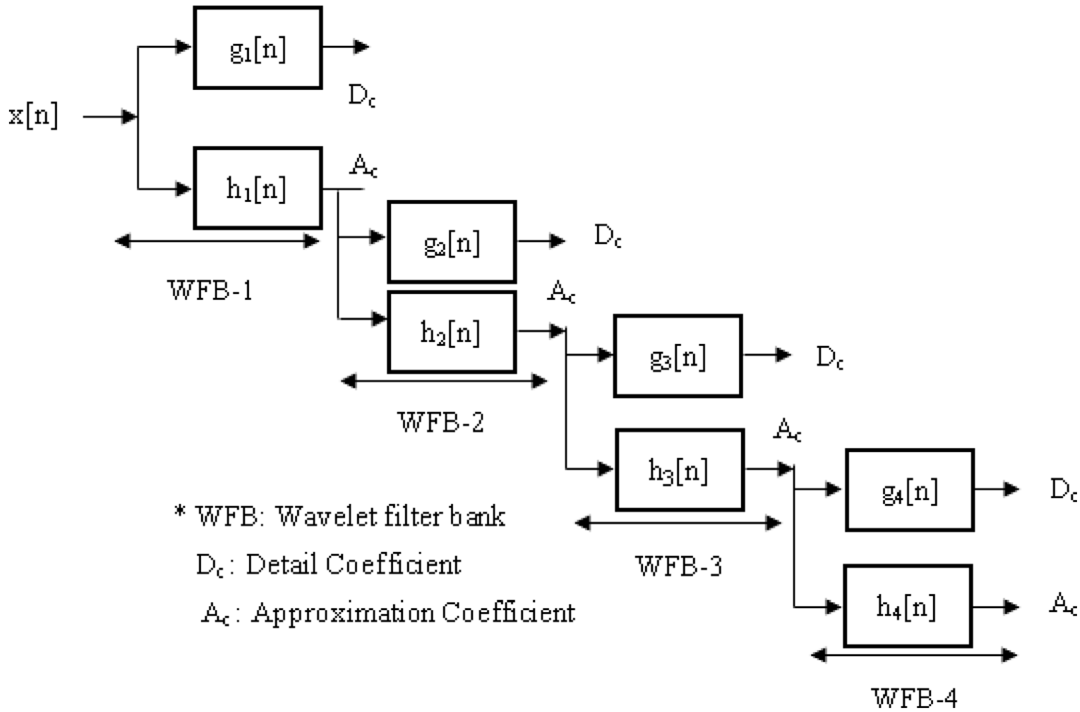

Fig. 4. Signal decomposition using SWT.

after filtering the noisy signal [18]. A ten-second recording with a sampling frequency of 360 Hz, 350 Hz, and 1000 Hz represents sample sizes of 3600, 2500, and 10000, respectively. The sample size is denoted by *N*. PRD percentage-root-mean-square difference (PRD) is calculated to check the distortion in the denoised signal as compared to the original signal, and is given by Eq. (12).

$$\mathrm{PRD} = 100 \times \sqrt{\frac{\sum_{n=1}^{N}\left(x\left(k\right)-\hat{x}\left(k\right)\right)^{2}}{\sum_{n=1}^{N}x^{2}\left(k\right)}} \tag{12}$$

RMSE is a root-mean-square-error, generally computed to check the variation between the actual signal and the denoised one. It is defined in Eq. (13) as follows:

$$\mathrm{RMSE} = \sqrt{\frac{1}{N}\sum_{n=1}^{N}\left(\hat{x}\left(k\right)-x\left(k\right)\right)^{2}} \tag{13}$$

A higher value of SNR represents the better quality of the denoised signal. In contrast, a corresponding minimum value of PRD and RMSE ensures the recovery of the original signal.

All the denoising techniques are plotted using the MIT-BIH arrhythmia database (*208* series of data). For analyzing critical cases, the input signal is made corrupted by adding a random noise source. In these figures, the '*Y*' axis represents the signal's amplitude in mV (millivolts), and the '*X*'-Axis represents the number of samples. The sampling frequency is 360 Hz. The denoising performance of various ECG denoising technique is evaluated using 208 series data from *physionet.org,* and the signal is shown in Fig. 5(a). ECG signal corrupted with a randomly generated noise source is shown in Fig. 5(b).

The ECG signal output after denoising using different ECG signal denoising techniques is shown in Fig. 6. Denoised ECG signal using lowpass filter based ECG denoising technique is shown in Fig. 6(a). As observed in Fig. 6(a), the noise present in the denoised ECG signal, even after filtering, degrades the SNR of the denoising algorithm.

Denoised ECG signal using highpass filter based ECG denoising technique is shown in Fig. 6(b). As observed in Fig. 6(b), there is still some noise present in the denoised ECG signal even after filtering, which degrades the SNR of the denoising algorithm. Denoised ECG signals using DWT, FDM, and EMD based ECG denoising techniques are shown in Figs. 6(c) through 6(e), respectively. It is observed from Figs. 6(c) through 6(e) that the use of DWT, FDM, and EMD disturb the shape of the ECG signal and hence, degrades the SNR improvement of the denoising algorithm.

The denoising performance of the stationary wavelet transform based ECG denoising technique is shown in Fig. 7. It is observed from Fig. 7 that the use of a stationary wavelet transform produces a clean ECG signal. Hence, the most considerable SNR improvement of the denoising algorithm is achieved.

Performance evaluation of the different ECG denoising techniques is as follows. Performance in terms of input SNR, and output SNR, of the different ECG signal denoising techniques are tabulated in Table 1. LPF and HPF denotes lowpass filter and highpass filter in all Tables. As observed from Table 1, the largest SNR improvement is in the range of 32 dB–45 dB, achieved using the SWT-based ECG signal denoising technique. Performance in terms of input SNR and output PRD of different ECG signal denoising techniques is discussed in Table 2.

As observed from Table 2, the lowest PRD value in the range of 0.094–0.758 is achieved using the SWT-based ECG signal denoising technique. Performance in terms of input SNR, RMSE of different ECG signal denoising technique is discussed in Table 3.

As observed in Table 3, the lowest RMSE in the range of 0.0006–0.0060 is achieved using the SWT-based ECG signal denoising technique. Tables 1 through 3 shows that the SWT technique provides maximum SNR and minimum PRD and RMSE compared to the other techniques. The average computation time of different ECG signal denoising techniques is listed in Table 4. The algorithms are implemented and computed on a computer with Intel Core i5 (7th generation), 8 GB memory, and 1 TB hard disk drive.

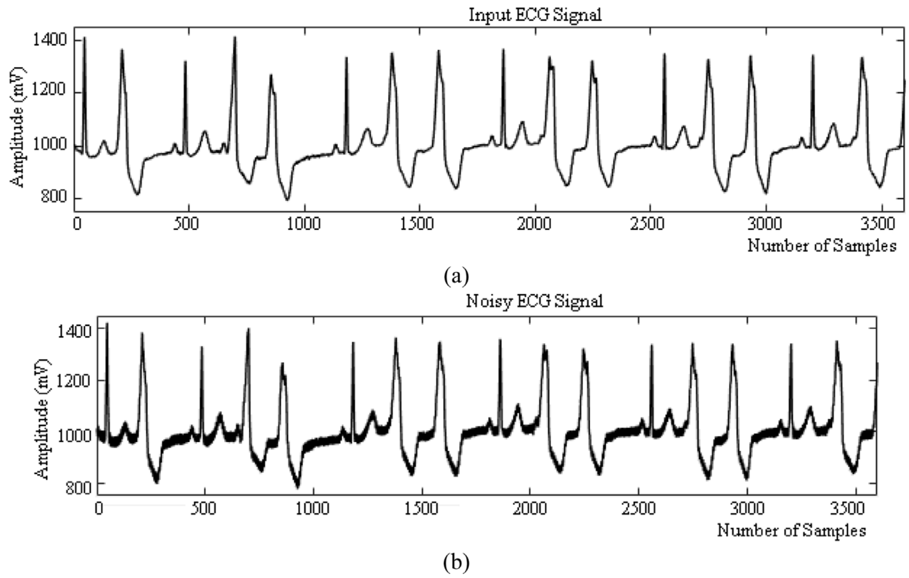

Fig. 5. (a) Input ECG Signal (208 series of data from *physionet.org*), (b) ECG signal corrupted with noise.

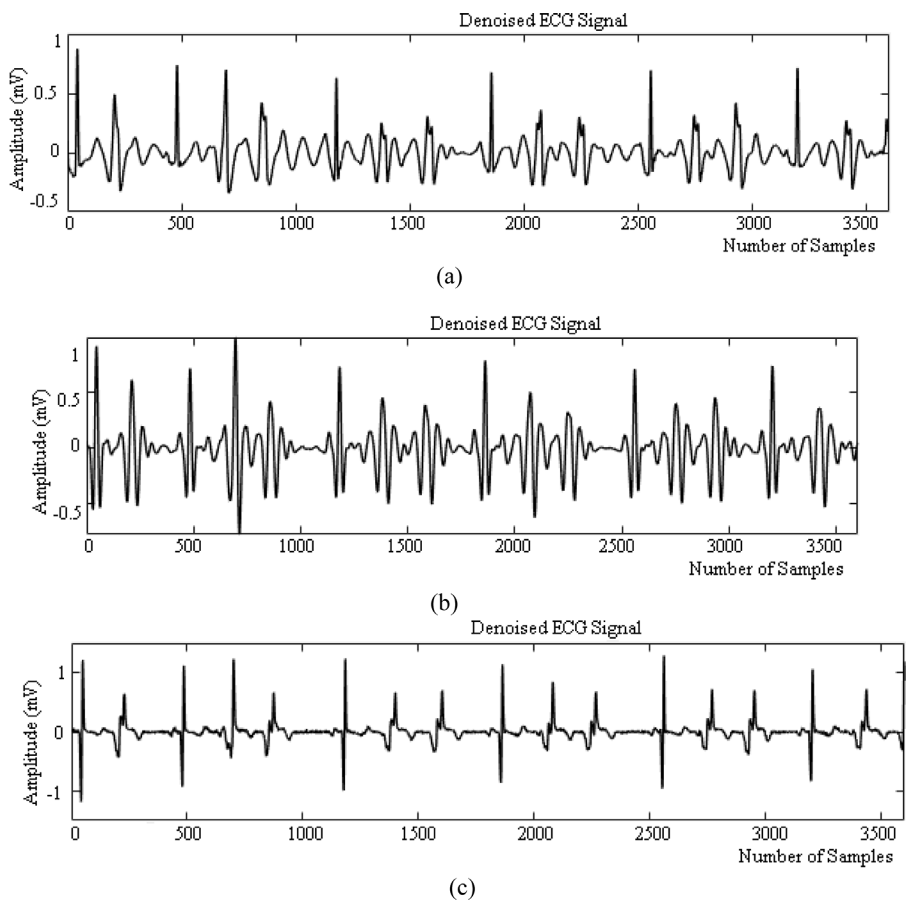

Fig. 6. ECG signal denoised using (a) a lowpass filter, (b) highpass filter, (c) discrete wavelet transform, (d) Fourier decomposition method (FIBF8 is denoised ECG signal), (e) Empirical decomposition method and corresponding IMFs and residual.

Table 4 shows that the SWT-based ECG denoising technique is computationally efficient compared to existing ECG signal denoising techniques.

5. Discussion

The study is extended to analyze the denoising performance of the proposed technique and other existing techniques. In this study, the input ECG signal is corrupted with noises of various magnitudes, and then different denoising techniques are applied.

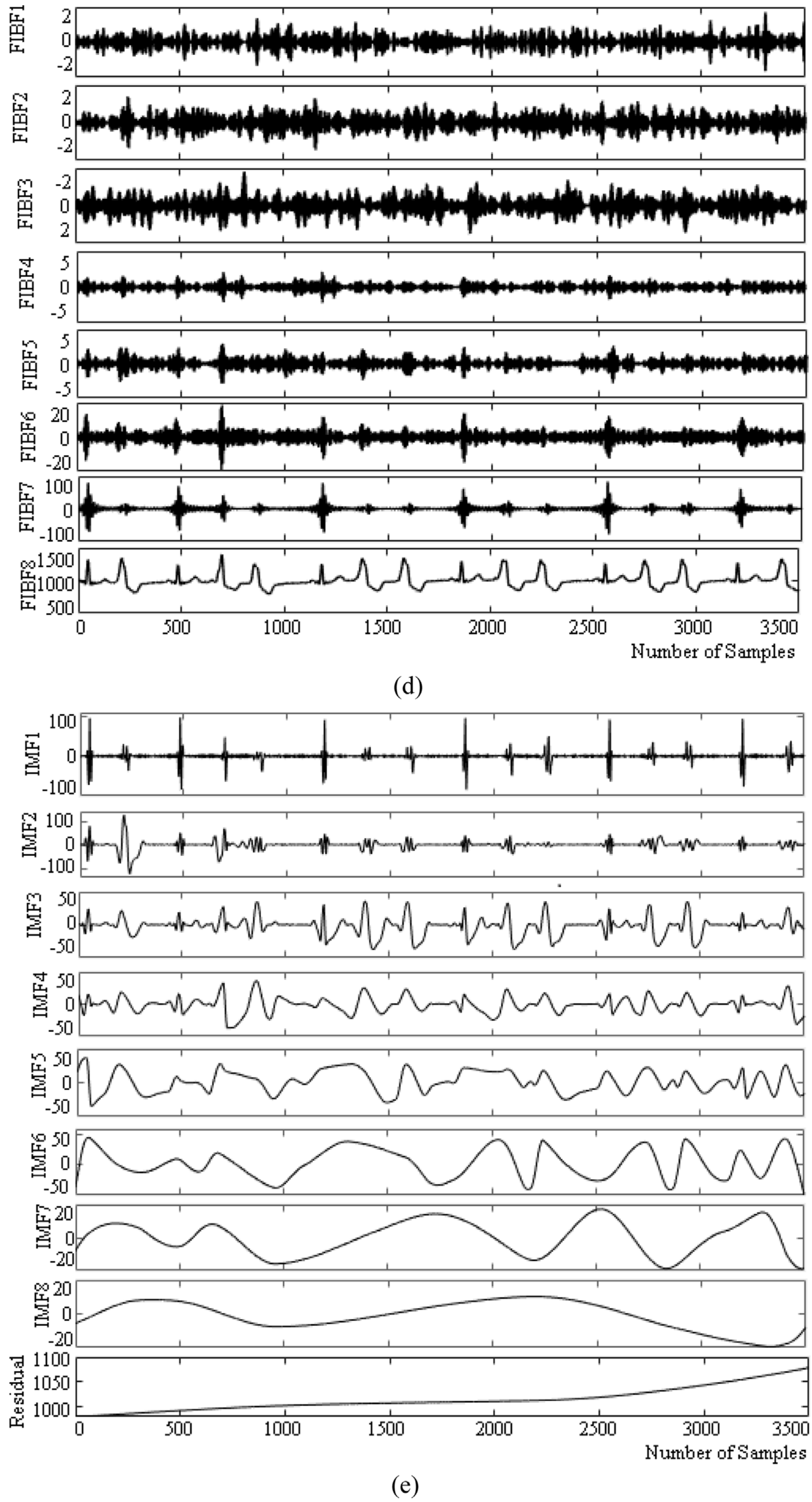

Fig. 6. (*continued*).

A comparison of various output performance parameters at different input SNR values is shown in Figs. 8 through 10. Fig. 8 compares the SNR values obtained by the SWT based ECG signal denoising technique with the existing techniques like lowpass filter, highpass filter, DWT, EMD, and FDM. As shown in Fig. 8, the performance of the SWT based ECG signal denoising method at an input SNR of −10 dB through 10 dB is remarkably better than the existing techniques. The highest output SNR ranging from 48.56 dB to 49.99 dB has been achieved by the SWT based ECG signal denoising technique on different input SNR levels. Figs. 9 and 10, respectively, compare the PRD and RMSE values obtained by the SWT based ECG signal denoising technique with

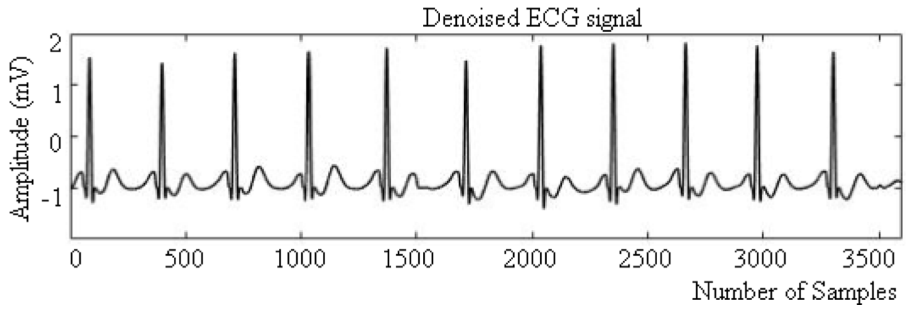

Fig. 7. Denoising performance of the stationary wavelet transform based ECG signal denoising technique.

Table 1
Input and output *SNR* of different ECG signal denoising techniques — evaluated on entire MIT-BIH arrhythmia database.

ECG record	Input SNR (dB)	Output performance evaluation parameters — SNR (dB)					
		LPF	HPF	DWT	FDM	EMD	SWT
100	14.32	33.97	32.78	38.18	26.90	34.96	49.35
101	13.31	29.54	31.66	37.54	29.14	54.70	46.42
102	14.59	30.42	30.81	39.42	27.63	34.68	48.54
103	14.50	29.80	27.42	37.70	30.81	32.56	50.39
104	15.41	27.27	29.74	38.28	31.45	31.97	43.56
105	13.31	33.50	33.54	39.46	32.33	34.50	46.58
109	15.93	27.47	30.79	39.96	33.72	37.89	50.30
112	15.27	30.17	26.97	37.81	32.61	45.01	47.37
117	14.69	29.43	29.39	38.52	34.83	38.65	49.57
118	11.97	25.42	31.42	37.60	35.23	37.47	54.66
123	14.70	27.60	29.97	40.17	34.77	39.33	53.74
200	9.40	34.40	27.27	41.11	26.91	44.47	53.31
205	21.39	29.85	25.24	39.79	30.42	51.98	54.03
213	12.32	24.91	30.38	34.13	32.24	34.25	52.26
221	14.58	30.54	29.95	38.80	28.72	39.78	53.00
231	14.22	27.53	30.59	39.38	33.71	36.92	52.66
234	15.13	27.90	26.11	40.76	30.83	32.03	32.03

Table 2
Obtained input SNR and output *PRD* using different ECG signal denoising techniques — evaluated on entire MIT-BIH arrhythmia database.

ECG record	Input SNR (dB)	Output performance evaluation parameters — PRD					
		LPF	HPF	DWT	FDM	EMD	SWT
100	14.32	0.290	0.417	0.417	0.502	3.475	0.254
101	13.31	0.828	0.857	0.984	1.003	0.320	0.758
102	14.59	0.383	0.421	0.416	0.736	3.165	0.357
103	14.50	0.166	0.659	0.141	0.429	3.488	0.092
104	15.41	0.209	0.758	0.204	0.383	1.776	0.199
105	13.31	0.377	0.556	0.421	0.659	2.611	0.409
109	15.93	0.195	0.723	0.213	0.799	2.531	0.214
112	15.27	0.207	0.691	0.267	0.824	3.037	0.198
117	14.69	0.311	0.834	0.121	0.718	2.313	0.141
118	11.97	0.518	0.911	0.474	0.738	3.017	0.451
123	14.70	0.371	0.703	0.173	0.819	2.823	0.086
200	9.40	0.613	0.829	0.502	0.837	0.971	0.313
205	21.39	0.293	0.637	0.217	0.678	0.971	0.161
213	12.32	0.286	0.721	0.353	0.703	2.666	0.294
221	14.58	0.145	0.593	0.249	0.801	1.139	0.121
231	14.22	0.138	0.545	0.107	0.794	2.819	0.094
234	15.13	0.634	0.687	0.335	0.925	3.389	0.395

the existing techniques like lowpass filter, highpass filter, DWT, EMD, and FDM. As shown in Figs. 9 and 10, the SWT-based ECG signal denoising method at an input SNR of −10 dB through 10 dB is remarkably better than the existing techniques. The lowest PRD ranging from 0.140 to 0.294 has been achieved by the SWT based ECG signal denoising technique on different input SNR levels. The lowest RMSE ranging from 0.0006 to 0.0029 has been achieved by the SWT based ECG signal denoising technique on different input SNR levels.

Table 1 shows that the performance of ECG signal denoising using lowpass filter shows significant improvement in SNR at the output, with a substantial improvement in *SNRimp*. Correspondingly PRD, RMSE is low, as discussed in Tables 2 and 3, respectively, indicating that the output signal is less distorted than the input signal. Since a lowpass filter can remove only high-frequency noises, it has a degraded SNR performance. On the other hand, as a highpass filter can only remove low-frequency signals, Table 1 indicates that the ECG signal denoising using a highpass filter has the lowest output SNR and highest RMSE, translating to more distortion in the output. A comparison between FDM and EMD ECG denoising techniques indicates that EMD is a better ECG denoising technique as EMD discards noise

Table 3
Obtained input SNR and RMSE using different ECG signal denoising techniques — evaluated on entire MIT-BIH arrhythmia database.

ECG record	Input SNR (dB)	Output performance evaluation parameters — RMSE					
		LPF	HPF	DWT	FDM	EMD	SWT
100	14.32	0.0008	0.0360	0.0012	0.0489	0.0026	0.0006
101	13.31	0.0016	0.0538	0.0018	0.0479	0.0031	0.0012
102	14.59	0.0015	0.0574	0.0016	0.0583	0.0029	0.0014
103	14.50	0.0013	0.0400	0.0015	0.0458	0.0035	0.0008
104	15.41	0.0021	0.0469	0.0019	0.0948	0.0048	0.0019
105	13.31	0.0008	0.0556	0.0009	0.0624	0.0017	0.0007
109	15.93	0.0023	0.0519	0.0023	0.0435	0.0036	0.0021
112	15.27	0.0023	0.0435	0.0026	0.0583	0.0035	0.0020
117	14.69	0.0024	0.0547	0.0007	0.0346	0.0035	0.0009
118	11.97	0.0046	0.0489	0.0040	0.0458	0.0051	0.0035
123	14.70	0.0025	0.0447	0.0011	0.0400	0.0030	0.0004
200	9.40	0.0008	0.0565	0.0006	0.0489	0.0004	0.0003
205	21.39	0.0016	0.0800	0.0011	0.0583	0.0007	0.0060
213	12.32	0.0072	0.0538	0.0077	0.0574	0.0103	0.0009
221	14.58	0.0013	0.0412	0.0016	0.0479	0.0015	0.0011
231	14.22	0.0018	0.0556	0.0012	0.0412	0.0020	0.0013
234	15.13	0.0020	0.0500	0.0016	0.0538	0.0020	0.0006

Table 4
Average computation time of different ECG signal denoising techniques.

Noise level (SNR_{in})	Average computation time in seconds					
	LPF	HPF	DWT	EMD	FDM	SWT
15 dB	3.65	3.37	4.28	4.96	5.00	3.06
10 dB	3.36	3.24	4.10	4.71	4.81	2.99
0 dB	2.99	3.02	3.99	4.25	4.77	2.88
−10 dB	3.11	3.19	4.06	4.39	4.83	2.93
−15 dB	3.26	3.22	4.21	4.56	4.88	2.96
Average	3.27	3.20	4.13	4.57	4.86	2.96

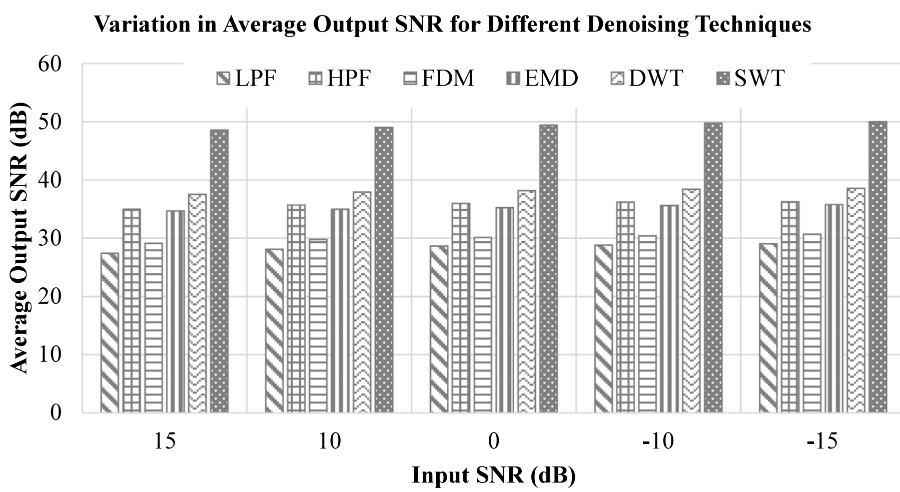

Fig. 8. Output SNR values obtained by the SWT based ECG signal denoising technique as compared to the existing methods.

from low-frequency components. A comparison of ECG signal denoising techniques based on EMD and DWT techniques indicates a better performance of the DWT based algorithms as EMD cannot effectively suppress noises with multiple frequency components. A comparison between the ECG denoising techniques based on DWT and SWT shows an improved denoising performance by the SWT denoising technique as SWT does not require the decimation of a signal is the case with DWT. Hence, it is evident that the SWT based ECG signal denoising technique is the best available ECG denoising technique.

As observed in Fig. 7, SWT results in a denoised ECG signal with high visual quality and preserves the ECG signal components. The other remarkable feature of the proposed denoising technique using SWT is that it retains the QRS complex's amplitude. In contrast, the existing denoising algorithms reduce the QRS complex's amplitude. Most of the ECG detection techniques alter the denoised ECG signal amplitude, while SWT does not change the amplitude of the denoised ECG signal. Thus, the SWT algorithm makes it more suitable for hardware implementation with low computational complexity since ECG denoising techniques like derivative followed by thresholding to enhance and detect R-peak and QRS Complex are not required. Hence SWT based denoising techniques can enable the ECG recording in noisy environments where the amplitude of the noise is high.

6. Conclusion

In this paper, a comparison between different ECG denoising techniques is performed to understand the numerically efficient denoising technique. All the ECG denoising techniques discussed

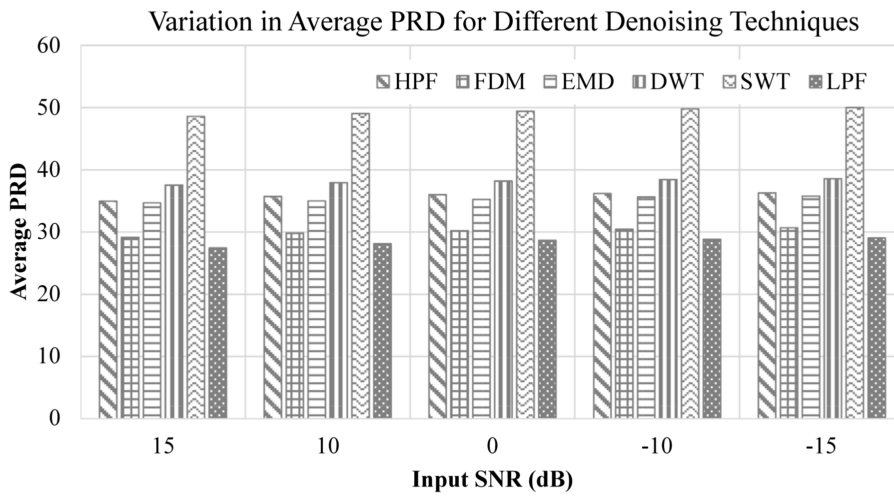

Fig. 9. Average PRD values obtained by the SWT based ECG signal denoising technique as compared to the existing methods.

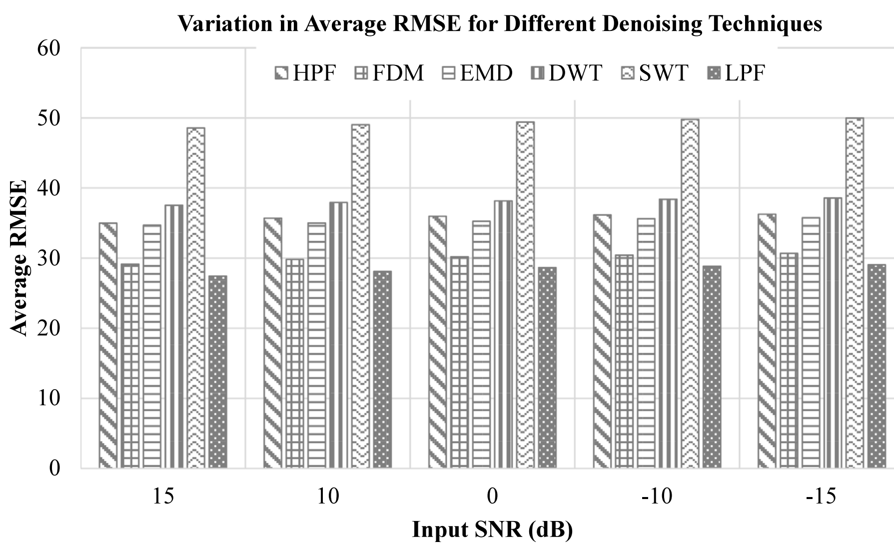

Fig. 10. Average RMSE values obtained by the SWT based ECG signal denoising technique as compared to the existing methods.

above are compared on different input and output performance evaluation parameters: SNR, PRD, and RMSE. SWT is an efficient and potential denoising method that can easily suppress noises like powerline interference and baseline wandering from a corrupted ECG signal. SWT is one of the best approaches which is used for non-stationary signals in real-time applications. This method showed better results by providing maximum SNR and minimum PRD, RMSE when compared to other ECG denoising techniques. An improvement of SNR between 28 dB–40 dB, and corresponding minimum output PRD and output RMSE are 0.092 and 0.0006, respectively are observed. These results proved that the denoised signal obtained is of very high quality and is least deviated from the original signal.

Further, analyzing results in more detail showed that denoising using SWT works as one of the most effective tools in the pre-processing of ECG signals. Due to the unique feature of retaining the amplitude after denoising, SWT can be used to realize hardware with low computational complexity to denoise ECG signals. In the future, SWT can be incorporated in newer techniques to achieve a hybrid model applicable for ECG signals and other biomedical signals as well.

Declaration of competing interest

The authors declare that they have no known competing financial interests or personal relationships that could have appeared to influence the work reported in this paper.

References

[1] Orlandic L, De Giovanni E, Arza A, Yazdani S, Vesin JM, Atienza D. Reward: Design, optimization, and evaluation of a real-time relative-energy wearable R-peak detection algorithm. In: 2019 41st annual international conference of the IEEE engineering in medicine and biology society. IEEE; 2019, p. 3341–7.
[2] Alberdi A, Aztiria A, Basarab A. Towards an automatic early stress recognition system for office environments based on multimodal measurements: A review. J Biomed Inform 2016;59:49–75.
[3] Berkaya SK, Uysal AK, Gunal ES, Ergin S, Gunal S, Gulmezoglu MB. A survey on ECG analysis. Biomed Signal Process Control 2018;43:216–35.
[4] Berwal D, Vandana CR, Dewan S, Jiji CV, Baghini MS. Motion artifact removal in ambulatory ECG signal for heart rate variability analysis. IEEE Sens J 2019;19(24):12432–42.
[5] Antman EM, Anbe DT, Armstrong PW, Bates ER, Green LA, Hand M, et al. ACC/AHA guidelines for the management of patients with ST-elevation myocardial infarction: A report of the American college of cardiology/American heart association task force on practice guidelines (committee to revise the 1999 guidelines for the management of patients with acute myocardial infarction). J Am Coll Cardiol 1999;44(3):E1–211.

[6] Sahambi JS, Tandon SN, Bhatt RK. Quantitative analysis of errors due to power-line interference and base-line drift in detection of onsets and offsets in ECG using wavelets. Med Biol Eng Comput 1997;35(6):747–51.

[7] Lenis G, Pilia N, Loewe A, Schulze WH, Dössel O. Comparison of baseline wander removal techniques considering the preservation of ST changes in the ischemic ECG: A simulation study. Comput Math Methods Med 2017. http://dx.doi.org/10.1155/2017/9295029.

[8] Asgari S, Mehrnia A. A novel low-complexity digital filter design for wearable ECG devices. PLoS One 2017;12(4):e0175139. http://dx.doi.org/10.1371/journal.pone.0175139.

[9] Jin Z, Dong A, Shu M, Wang Y. Sparse ECG denoising with generalized minimax concave penalty. Sensors 2019;19(7):1718.

[10] Chen B, Li Y, Cao X, Sun W, He W. Removal of power line interference from ECG signals using adaptive notch filters of sharp resolution. IEEE Access 2019;7:150667–76.

[11] Appathurai A, Carol JJ, Raja C, Kumar SN, Daniel AV, Malar AJ, et al. A study on ECG signal characterization and practical implementation of some ECG characterization techniques. Measurement 2019;147:106384.

[12] Poungponsri S, Yu XH. An adaptive filtering approach for electrocardiogram (ECG) signal noise reduction using neural networks. Neurocomputing 2013;117:206–13.

[13] Mohebbian MR, Alam MW, Wahid KA, Dinh A. Single channel high noise level ECG deconvolution using optimized blind adaptive filtering and fixed-point convolution kernel compensation. Biomed Signal Process Control 2020;57:101673. http://dx.doi.org/10.1016/j.bspc.2019.101673.

[14] Rakshit M, Das S. An efficient ECG denoising methodology using empirical mode decomposition and adaptive switching mean filter. Biomed Signal Process Control 2018;40:140–8.

[15] Kumar S, Panigrahy D, Sahu PK. Denoising of electrocardiogram (ECG) signal by using empirical mode decomposition (EMD) with non-local mean (NLM) technique. Biocybern Biomed Eng 2018;38(2):297–312.

[16] Kumar A, Komaragiri R, Kumar M. Heart rate monitoring and therapeutic devices: A wavelet transform based approach for the modeling and classification of congestive heart failure. ISA Trans 2018;79:239–50.

[17] Kumar A, Komaragiri R, Kumar M. Design of wavelet transform based electrocardiogram monitoring system. ISA Trans 2018;80:381–98.

[18] Kumar A, Komaragiri R, Kumar M. From pacemaker to wearable: Techniques for ECG detection systems. J Med Syst 2018;42(2):34.

[19] Kumar A, Kumar M, Komaragiri R. Design of a biorthogonal wavelet transform based R-peak detection and data compression scheme for implantable cardiac pacemaker systems. J Med syst 2018;42(6):102.

[20] Berwal D, Kumar A, Kumar Y. Design of high performance QRS complex detector for wearable healthcare devices using biorthogonal spline wavelet transform. ISA Trans 2018;81:222–30.

[21] Kumar A, Berwal D, Kumar Y. Design of high-performance ECG detector for implantable cardiac pacemaker systems using biorthogonal wavelet transform. Circuits Systems Signal Process 2018;37(9):3995–4014.

[22] Vázquez RR, Velez-Perez H, Ranta R, Dorr VL, Maquin D, Maillard L. Blind source separation wavelet denoising and discriminant analysis for EEG artefacts and noise cancelling. Biomed Signal Process Control 2012;7(4):389–400.

[23] Singhal A, Singh P, Fatimah B, Pachori RB. An efficient removal of power-line interference and baseline wander from ECG signals by employing Fourier decomposition technique. Biomed Signal Process Control 2020;57:101741. http://dx.doi.org/10.1016/j.bspc.2019.101741.

[24] Van Alste JA, Schilder TS. Removal of base-line wander and power-line interference from the ECG by an efficient FIR filter with a reduced number of taps. IEEE Trans Biomed Eng 1985;BME-32(12):1052–60.

[25] Wang J, Ye Y, Pan X, Gao X, Zhuang C. Fractional zero-phase filtering based on the Riemann–Liouville integral. Signal Process 2014;98:150–7.

[26] Liang H, Lin QH, Chen JD. Application of the empirical mode decomposition to the analysis of esophageal manometric data in gastroesophageal reflux disease. IEEE Trans Biomed Eng 2005;52(10):1692–701.

[27] Kim H, Kim S, Van Helleputte N, Berset T, Geng D, Romero I, et al. Motion artifact removal using cascade adaptive filtering for ambulatory ECG monitoring system. In: 2012 IEEE biomedical circuits and systems conference. IEEE; 2012, p. 160–3.

[28] Bozkurt A, Gilmour Jr RF, Sinha A, Stern D, Lal A. A insect–machine interface based neurocybernetics. IEEE Trans Biomed Eng 2009;56(6):1727–33.

[29] Weaver C, Von Der Groeben J, Mantey P, Toole J, Cole C, Fitzgerald J, et al. Digital filtering with applications to electrocardiogram processing. IEEE Trans Audio Electroacoust 1968;16(3):350–91.

[30] Malghan PG, Hota MK. A review on ECG filtering techniques for rhythm analysis. Res Biomed Eng 2020;19:1–6. http://dx.doi.org/10.1007/s42600-020-00057-9.

[31] Pei SC, Tseng CC. IIR multiple notch filter design based on allpass filter. IEEE Trans Circuits Syst II 1997;44(2):133–6.

[32] Kim KJ, Ku JH, Kim IY, Kim SI, Nam SW. Notch filter design using the α-scaled sampling kernel and its application to power line noise removal from ECG signals. In: 2007 international conference on control, automation and systems. IEEE; 2007, p. 2415–8.

[33] Widrow B, Glover JR, McCool JM, Kaunitz J, Williams CS, Hearn RH, et al. Adaptive noise cancelling: Principles and applications. Proc IEEE 1975;63(12):1692–716.

[34] Buxi D, Berset T, Hijdra M, Tutelaers M, Geng D, Hulzink J, et al. Wireless 3-lead ECG system with on-board digital signal processing for ambulatory monitoring. In: 2012 IEEE biomedical circuits and systems conference. IEEE; 2012, p. 308–11.

[35] Leavey CM, James MN, Summerscales J, Sutton R. An introduction to wavelet transforms: A tutorial approach. Insight, Non-Destr Test Cond Monit 2003;45(5):344–53. http://dx.doi.org/10.1784/insi.45.5.344.52875.

[36] Zhang Z, Telesford QK, Giusti C, Lim KO, Bassett DS. Choosing wavelet methods filters and lengths for functional brain network construction. PLoS One 2016;11(6):e0157243.

[37] Seljuq U, Himayun F, Rasheed H. Selection of an optimal mother wavelet basis function for ECG signal denoising. In: 17th IEEE international multi topic conference 2014. IEEE; 2014, p. 26–30.

[38] Strasser F, Muma M, Zoubir AM. Motion artifact removal in ECG signals using multi-resolution thresholding. In: 2012 proceedings of the 20th European signal processing conference. IEEE; 2012, p. 899–903.

[39] Huang NE, Shen Z, Long SR, Wu MC, Shih HH, Zheng Q, et al. The empirical mode decomposition and the Hilbert spectrum for nonlinear and non-stationary time series analysis. Proc R Soc Lond Ser A Math Phys Eng Sci 1998;454(1971):903–95. http://dx.doi.org/10.1098/rspa.1998.0193.

[40] Pal S, Mitra M. Empirical mode decomposition based ECG enhancement and QRS detection. Comput Biol Med 2012;42(1):83–92.

[41] Singh P, Joshi SD, Patney RK, Saha K. The Fourier decomposition method for nonlinear and non-stationary time series analysis. Proc R Soc Lond Ser A Math Phys Eng Sci 2017;473(2199):20160871.

[42] [online]. Available: https://archive.physionet.org/cgi-bin/atm/ATM. [Accessed on 25, November 2020].

[43] Subramanian B. ECG signal classification and parameter estimation using multiwavelet transform. Biomed Res 2016;28(7):3187–93.

[44] Kumar A, Komaragiri R, Kumar M. Design of efficient fractional operator for ECG signal detection in implantable cardiac pacemaker systems. Int J Circuit Theory Appl 2019;47(9):1459–76.

[45] Alfaouri M, Daqrouq K. ECG signal denoising by wavelet transform thresholding. Am J Appl Sci 2008;5(3):276–81.

[46] Polikar R. The story of wavelets. In: Physics and modern topics in mechanical and electrical engineering. World Scientific and Eng. Society Press; 1999, p. 192–7.

[47] Moody GB, Mark RG. The impact of the MIT-BIH arrhythmia database. IEEE Eng Med Biol Mag 2001;20(3):45–50.

[48] Moody GB, Muldrow W, Mark RG. A noise stress test for arrhythmia detectors. Comput Cardiol 1984;11(3):381–4.

[49] Bousseljot R, Kreiseler D, Schnabel A. Nutzung der EKG-Signaldatenbank CARDIODAT der PTB über das Internet. Biomed Eng 1995;40(s1):317–8.